J. Phys. Chem. Solids Vol. 41, pp. 31–41
Pergamon Press Ltd., 1980. Printed in Great Britain

STUDY OF PHASE TRANSITIONS AND PROPERTIES OF TETRAGONAL (Pb, La) (Zr, Ti)O_3 CERAMICS—III

TRANSITIONS INDUCED BY ELECTRIC FIELDS

C. G. F. STENGER and A. J. BURGGRAAF
Twente University of Technology, Department of Chemical Engineering, Laboratory of Inorganic Chemistry and Materials Science, P.O. Box 217, 7500 AE Enschede, The Netherlands

(*Received* 30 *October* 1978; *accepted in revised form* 4 *May* 1979)

Abstract—The phase diagram of electrically poled, tetragonal *PLZT* materials has been investigated. In the higher La concentration range, a tetragonal, so-called β-phase occurs, which has no clear FE properties. The transition to the FE_t phase has first order character and takes place only after a strong electric field has been applied to the material. The energetics of the $\beta_t \leftrightarrows FE_t$ transition were investigated in several ways. The heat-effects associated with this transition have a small value of 6-20 cal/mol, dependent on composition. The transition $\beta_t \leftrightarrows FE_t$ is accompanied by a relatively large activation energy ΔG_2. The $\Delta G_2(T)$ curve shows a minimum for materials, which do not show a spontaneous transition to the FE_t phase. This minimum value of ΔG_2 (1–2.5 cal/mol) is large in comparison to the average thermal energy kT and prevents the spontaneous transition from the β_t phase to the FE_t phase.

1. INTRODUCTION

Phase relations in *PLZT* 8/65/35 have been investigated extensively by several authors [1–5]. At high temperatures the material is paraelectric (*PE*) with a cubic symmetry. On lowering the temperature, a broadened anomaly in the permittivity curve is observed, however a crystallographic transition is absent and the material is (pseudo) cubic† at low temperatures. A ferroelectric orthorhombic phase can be induced by the addition of electrical or mechanical energy. This latter transition is reversible at temperatures above a certain temperature T_p and non reversible at temperatures below T_p.

A similar behaviour has been reported for the more Ti rich, tetragonal *PLZT* materials. A study of the phase relations in thermally depoled *x*/30/70 materials has been reported in Part I of this paper. Contrary to *PLZT* 8/65/35, in these materials a spontaneous transition to a tetragonal phase occurs at all La concentrations. However at high La-concentrations, the tetragonal phase has no ferroelectric properties [6, 7] and this so called β_t phase can be converted to the FE_t phase by applying an electric field to the material [7]. The character of the (pseudo) cubic phase in *PLZT x*/65/35 materials and the β_t phase in *PLZT x*/55/45 and *PLZT x*/30/70 materials is not yet clear, but the most current idea is the short range order model, discussed in Part II of this paper.

The transition $\beta \rightarrow FE_t$ is accompanied by: (i) a jump in polarization, (ii) an anomalous change of physical properties such as ϵ', ϵ'', light scattering, etc. (iii) an exothermic heat effect.

In the literature these facts have been put forward as criteria for the short range order→long range order transition. The aim of this paper is to report on phase relations in poled tetragonal *PLZT* materials. Experimental results and the phase diagram (*T*-*x* plot) for poled *x*/30/70 materials will be discussed in Sections 2 and 3.1 respectively.

A comparison with the phase diagram for thermally depoled material will show, that the FE_t phase field grows at the expense of the β_t phase field. Furthermore it will be shown, that the transition $FE_t \rightarrow \beta_t$ has first order character and takes place at a relative sharply defined temperature T_p.

The electrical induction of the FE_t phase and the energetics of the transition $\beta_t \rightarrow FE_t$ will be discussed in Sections 2.2–3.4. The results are consistent with the short range order model. It will be made clear in these sections, that the fact, that the transition $\beta_t \rightarrow FE_t$ does not occur spontaneously for materials with a high La content, is the result of an activation energy, which is high in comparison with the average thermal energy kT. Finally in Section 3.6 a comparison with other *PLZT* materials will be made which leads to the conclusion, that the electrical induction of a FE phase is a general phenomenon for *PLZT* materials with a relative high La content.

2. EXPERIMENTAL METHODS AND RESULTS

The preparation of the *PLZT* materials and the experimental equipment for capacitance, X-ray and *DSC* measurements is described in [6].

2.1 *Polarization measurements*

By means of a modified Sawyer–Tower circuit, *EP* hysteresis loops were obtained at a frequency of 0.05 Hz. A typical sequence of *EP* hysteresis loops as a function of temperature is shown in Fig. 1. At low temperatures a square loop is observed, which changes into a double

†In a private communication, Sternberg (Latvian State University, Riga, USSR) reported, that at low temperatures *PLZT* 8/65/35/ shows a slight deviation from the cubic symmetry. This is in disagreement with the results of Keve *et al.* [2].

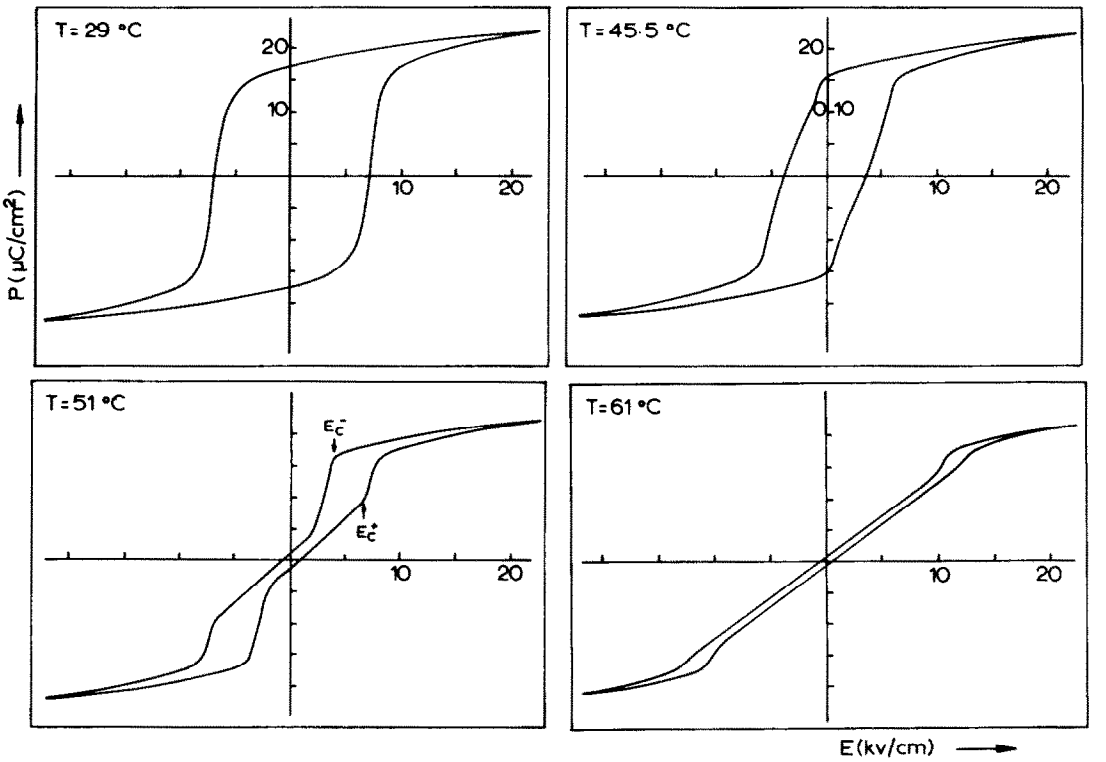

Fig. 1. EP hysteresis loops for *PLZT* 17/30/70 material at different temperatures.

loop at increasing temperature. At still higher temperatures a so-called slim loop is found, which gradually approaches linear dielectric behaviour.

Remanent polarization as a function of temperature was obtained from these *EP* hysteresis loops and is shown in Fig. 2 for several *x*/30/70 materials. All materials show a loss of overall polarization at a temperature T_p. Although some polarization is retained above T_p, the temperature T_p is sharply defined in nearly all cases. In Fig. 3, virgin† *EP* curves are shown for several *PLZT* materials at different temperatures ($T < T_p$). In our opinion the kinks in the virgin *EP* curves for *PLZT* 17/30/70 and 20/30/70 at *a* and *b* are indicative for a phase transition. This phenomenon will be discussed extensively in Section 3.

†A material is in its virgin state or thermally depoled state after heating to a temperature far above the Curie temperature, followed by slowly cooling. In this way the memory of the electrical history of the material is completely removed.

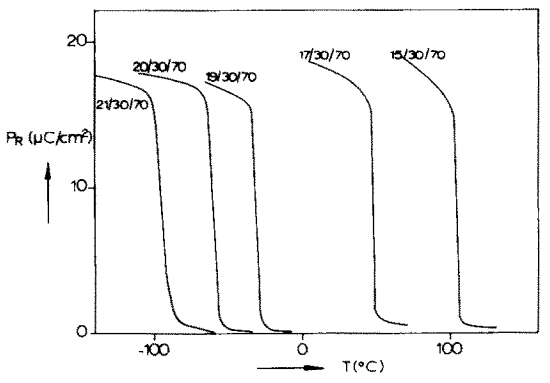

Fig. 2. Remanent polarization as function of temperature for several *PLZT* x/30/70 materials.

2.2 *Capacitance measurements*

In the lower La concentration range (*x*/30/70 materials with $x < 16$ at % La) the ϵ' (T) and ϵ'' (T) curves of poled and thermally depoled materials are equal. The temperature T_p is coincident with the temperature, where the dielectric constant is at maximum (T_c) and temperature where the dielectric loss is at maximum (T_b). Increasing the La content, however, leads to a completely different behaviour. The temperature dependence of the dielectric constant of 17/30/70 and 20/30/70 materials is shown in Fig. 4. Two different starting conditions, poled and thermally depoled, are shown in curves (a) and (b) respectively. At temperatures $T < T_p$, the dielectric constant of the poled material is much lower than that of the thermally depoled material. The difference increases with increasing temperature.

However at temperature T_p the dielectric constant of the poled material shows a sudden increase, whereas in thermally depoled material such an increase is absent. Once depoled at the temperature T_p, no further difference could be observed between poled and thermally depoled material on heating or cooling. The broadened maximum of the dielectric constant occurs at a *higher* temperature (called T_c') than T_p in all cases and the temperature difference between T_p and T_c' *increases* rapidly with *increasing* La content (Table 1). Alternating

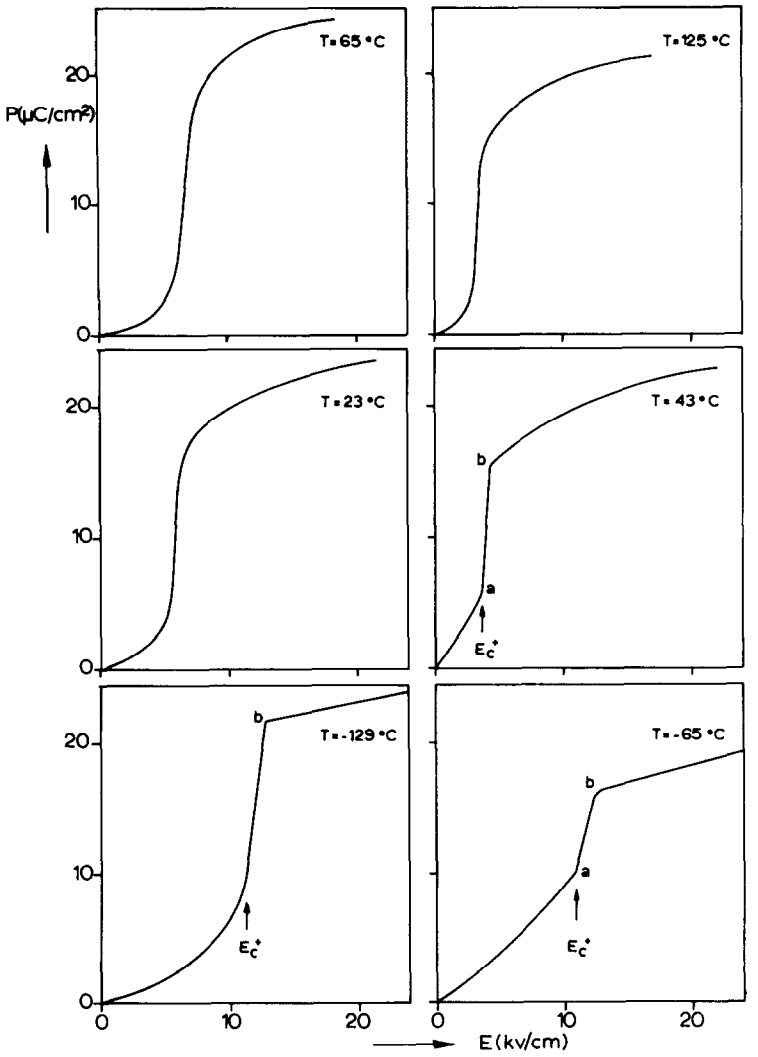

Fig. 3. Virgin EP curves for *PLZT x*/30/70 materials with $x = 14$ at % La (upper figures), $x = 17$ at % La (middle figures) and $x = 20$ at % La (bottom figures).

current depoled† material behaves in the same way as poled material.

2.3 *DSC measurements*

For *x*/30/70 materials with a low La content ($x < 16$ at % La) a latent heat effect is observed at a temperature T_t, both for poled and thermally depoled material. The magnitude of this heat effect is more or less equal in both cases. Poled and a.c. depoled materials in the higher La concentration range ($x > 16$ at % La) show a latent heat at the temperature T_p. The magnitude of this heat effect decreases linearly with increasing La content. For *PLZT x*/30/70 material with $x > 20$ at % La the heat effect vanishes, apparently because of its small value. It should be remarked, that the heat effects for materials with $x > 16$ at % La are very small and close to the sensitivity limit of our *DSC* equipment. Only the fact, that sharp *DSC* peaks were observed, made it possible to calculate values for the transition heat.

In Table 1 values of ΔH and ΔS for the transition $\beta \leftrightarrows$ FE are presented. ΔS was calculated from the equation $\Delta S = \Delta H / T_p$.

2.4 *X-Ray measurements*

X-Ray diffraction patterns were made at room temperature from poled and thermally depoled ceramic discs having a diameter of about 15 mm. Removable silver paste electrodes were used for the poling procedure. In all cases, poling resulted in a strongly increased intensity of *hkl* reflections with $1 > h + k$.

This result is expected because of the preferred orientation of the tetragonal axes in the poled material. However neither a change in symmetry nor a significant change in the *c*/*a* ratio could be observed in *PLZT* 17/30/70 and 11/55/45 materials due to poling (thermally depoled 17/30/70 is FE, thermally depoled 11/55/45 is a β-phase material at room temperature).

†A material can be a.c. depoled by continuously reducing the magnitude of the a.c. field strength which was initially equal to the maximum field used in hysteresis loop measurements.

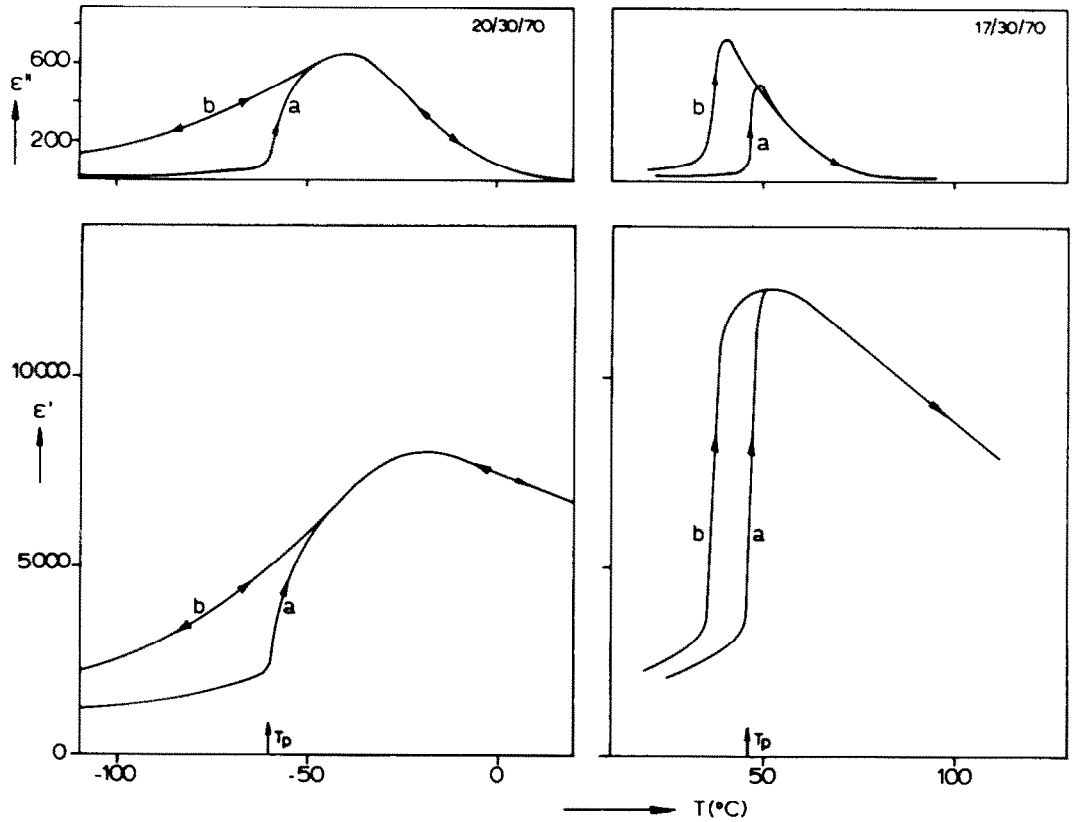

Fig. 4. Permittivity curves for thermally depoled (b) and poled (a) *PLZT* 17/30/70 and *PLZT* 20/30/70.

Finally it must be kept in mind that the crystallographic tetragonal→cubic transition takes place around or above the temperature where the dielectric constant is at maxinum [6].

This leads to the conclusion, that if the temperature T_p is indicative for a phase transition, this will be a tetragonal→tetragonal transition.

3. DISCUSSION

3.1 *Phase diagram for poled material*

The experiments, described above, strongly suggest that the depoling observed for materials with a high La content at temperature T_p is in fact a phase transition, but one which is not reversible on cooling. This necessarily implies, that thermally depoled materials with a

Table 1. Transition temperatures and thermodynamic quantities for the transitions in some tetragonal *PLZT* materials. Thermodynamic quantities were measured on poled samples†

material	T'_c (°C) at 10kHz	T_p (°C)	T_o (°C)	ΔH_{dsc} (cal/mol)	ΔS_{dsc} (cal/molK)	ΔS_{hyst} (cal/molK)	transition at T_p
12/30/70	191	194		26	0.06		FE→PE
14/30/70	130	135		24	0,06		FE→PE
15/30/70	105	104	97	23	0,06	0,06	FE→PE
16/30/70	85	80		21	0,06		FE→β
17/30/70	52	47	35	18	0,06	0,05	FE→β
18/30/70	33	14		16	0,06		FE→β
19/30/70	-4	-31	-43	13	0,05	0,04	FE→β
20/30/70	-19	-61	-80	10	0,05	0,05	FE→β
21/30/70	-32	-96	-127			0,04	FE→β
10/55/45	118	90					FE→β
11/55/45	80	48	33	12	0,05	0,04	FE→β
12/55/45	64	11					

†T'_c: Temperature where the dielectric constant is at maximum.
T_p: See text.
ΔH_{dsc}: Transition enthalpy, as measured by means of a *DSC* equipment.
ΔS_{dsc}: Transition entropy, calculated from $\Delta S = \Delta H_{dsc}/T_p$
ΔS_{hyst}: Transition entropy, calculated from double EP hysteresis loops.

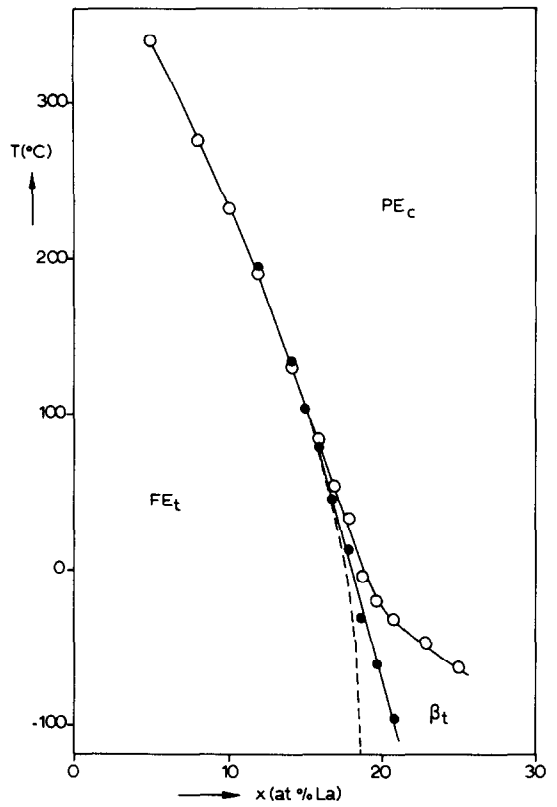

Fig. 5. Phase diagram for poled *PLZT x*/30/70 materials dotted line gives the transition $FE_t \rightarrow \beta_t$ in thermally depoled material.

high La content undergo a non-reversible phase transition to a FE phase on poling at temperatures below T_p.

We propose a phase diagram for poled *PLZT x*/30/70 materials as shown in Fig. 5. In the lower La concentration range, the situation is relative simple and equals the situation for a thermally depoled material [6]. The first order transition $FE_t \rightarrow PE_c$ takes place at temperature T_c' (ϵ at maximum) = T_b (ϵ'' at maximum) = T_t (*DSC* anomaly) = T_p (disappearance of remanent polarization) = T_x (crystallographic transition). All these temperatures are coincident in this La concentration range. Increasing the La content finally leads to a difference in behaviour of thermally depoled and poled material. Compared with the phase diagram for thermally depoled material, the diagram for poled materials shows an extended FE phase field. The β phase field on the other hand decreases. The (sharp) $FE_t \rightarrow \beta_t$ transition occurs at temperature T_p (disappearance of remanent polarization, sharp increase of ϵ' and ϵ'', latent heat effect), whereas the diffuse transition $\beta_t \rightarrow PE_c$ around the temperature T_c' (maximum ϵ') has been discussed in full detail in [6].

The transition $FE_t \rightarrow \beta_t$ has first order character, which can be deduced from the following:

—a latent heat is observed at the transition

—double EP hysteresis loops are observed at temperatures $T > T_p$. The FE character of the low temperature electrical induced phase becomes evident, in the first place from the observed square hysteresis loops and secondly from the fact that application of a bias field to the material results in an increase of temperature T_p. This is the theoretically expected result for a transition where a FE phase disappears [8].

3.2 EP *hysteresis measurements*

Virgin EP curves (Fig. 3) show a more or less normal domain orientation at all temperatures in the case of *PLZT* 14/30/70, which confirms the FE character of the thermally depoled material at $T < T_p$. On the other hand, virgin EP curves of *PLZT* 20/30/70 clearly indicate the induction of the FE phase from the thermally depoled material at all temperatures where $T < T_p$. At a certain critical field strength E_c^+ an FE phase is induced†. This transition is accompanied by kinks at *a* and *b* in the virgin EP curve and by a sharp change in other properties (strong decrease of ϵ' and ϵ'' etc. see also [7]).

PLZT 17/30/70 and 18/30/70 materials show an intermediate behaviour. Both domain orientation and phase transition behaviour, dependent on temperature, can be seen in the virgin EP hysteresis loops. In a temperature region not too far below temperature T_p a phase transition behaviour is observed in the virgin EP curves, which is in accordance with the proposed phase diagrams for poled and thermally depoled material. At lower temperatures, thermally depoled material undergoes a spontaneous transition to an FE phase and in the virgin EP curves only domain orientation behaviour is observed. In the EP hysteresis loops, shown in Fig. 1, the critical fields E_c^+ and E_c^- are also defined.

The transition $\beta_t \rightarrow FE_t$ occurs at the field E_c^+, whereas at the field E_c^-, the opposite transition occurs. The temperature dependence of these critical fields for several materials is given in Fig. 6. It can be seen from this figure, that the transition $\beta_t \rightarrow FE_t$ in *PLZT* 17/30/70 shows a rather large thermal hysteresis.

In the case of *PLZT* 20/30/70, hysteresis in a classical sense is absent. It can be seen from Fig. 6, that the critical field E_c^+ exhibits a broad minimum. At low temperatures, the critical field E_c^+ *increases*. This means that in zero or low field ($E < 8 kV/cm$), a spontaneous $\beta_t \rightarrow FE_t$ transition does not occur. In high fields ($E > 8 kV/cm$) a more or less normal thermal hysteresis will be observed. This is illustrated in Fig. 6. At a field strength of 10 kV/cm, the thermal hysteresis for the transition $\beta_t \leftrightarrows FE_t$ will be $T_a - T_b$.

From the double hysteresis loops an estimation of the free enthalpy difference between the FE_t and β_t phases can be obtained. This is illustrated in Fig. 7. Since hysteresis is observed in the EP curves, the real equilibriumcurve for the field enforced transition is assumed to be represented by the line ABC in Fig. 7. The dashed line ABC in this figure was drawn in such a way, as to divide the area enclosed by the hysteresis loop into two equal parts. The area ABCE represents the transition

†Especially at temperatures $T \ll T_p$ it is doubtful if the transition $\beta \rightarrow FE$ occurs at a sharply defined field strength, since at low temperatures a clear kink at the start of the transition (point *a* in Fig. 3.) is not observed. However, the sharp kink at point *b* remains at all temperatures.

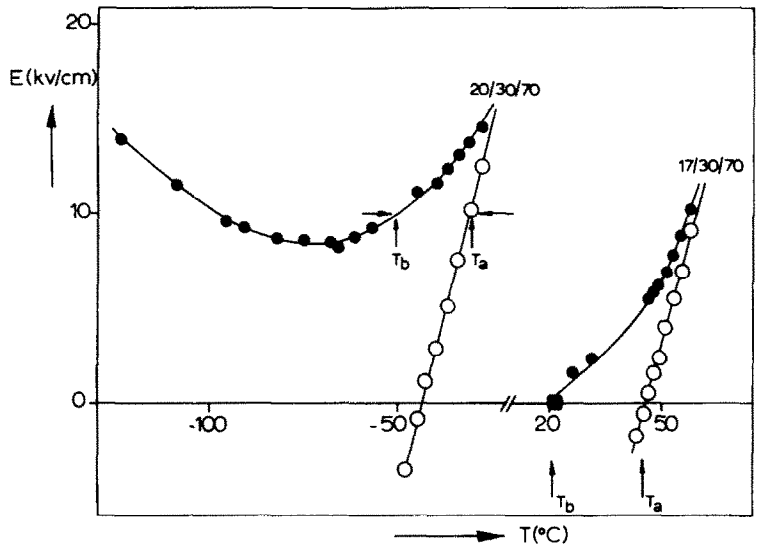

Fig. 6. Critical field E_c^+ and E_c^- as function of temperature for *PLZT* 17/30/70 and *PLZT* 20/30/70. Open circles: E_c^-, closed circles: E_c^+, closed square: transition temperature as determined from zero field permittivity curve (see [6]).

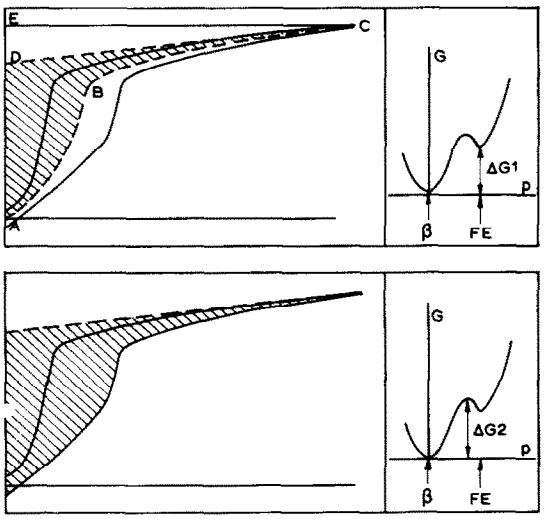

Fig. 7. Determination of the transition free enthalpy ΔG_1 and the activation energy ΔG_2 from the double hysteresis loops.

free enthalpy for the transition $\beta_t \rightarrow FE_t$. However a correction for the reversibly stored dielectric energy should be made. Theerfore the more or less linear ferroelectric part of the hysteresis loop is extrapolated back to the P axis (line DC). Now the dielectric energy is given by the area *DCE*, whereas the transition-free enthalpy ΔG_1 for the transition $\beta_t \rightarrow FE_t$ is given by the crosshatched area ABCD. It should be kept in mind however, that the transition-free enthalpy from the β_t phase to the *poled* FE_t phase is determined in this way.

A correction for the energy involved in the domain orientation process has not been performed.

In all cases a linear relationship between ΔG_1 and T is observed (Fig. 8). Extrapolating the $\Delta G_1(T)$ curve back to the T axis, yields the temperature T_0, where the transition should take place.

However, as will be made clear, a large activation energy will prevent the spontaneous occurence of the transition $\beta_t \rightarrow FE_t$ in materials with a high La content. The slope $\alpha = (\partial \Delta G_1 / \partial T)$ of the curve equals the tran-

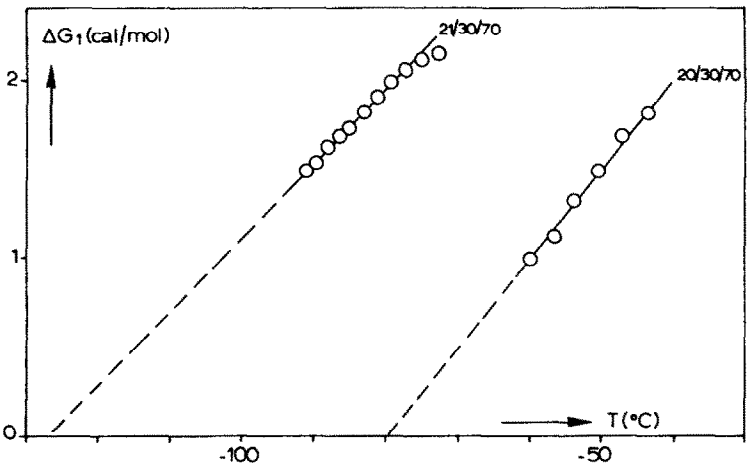

Fig. 8. Transition free enthalpy ΔG_1 as function of temperature for *PLZT* 20/30/70 and *PLZT* 21/30/70.

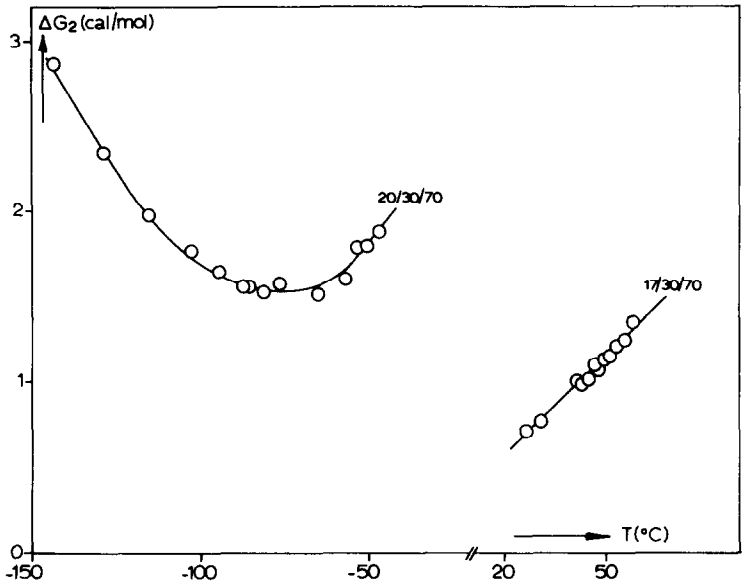

Fig. 9. Activation energy ΔG_2 as function of temperature for *PLZT* 17/30/70 and *PLZT* 20/30/70.

sition entropy for the transition $\beta_t \rightarrow FE_t$. In Table 1 the transition temperatures as obtained from different measurements, together with the results of the thermal measurements, are presented. From this table two striking facts should be observed:

(a) A large difference between the theoretical transition temperature T_0 and the experimental transition temperature T_p is observed. This difference increases with increasing La content.

(b) The values for the entropy differences between the Fe_t and β_t phases as obtained by different techniques, are almost equal.

In the calculations of ΔS from the double hysteresis loops, errors will result from the facts that the curve ABC in Fig. 7 is only an approximation of the true equilibrium curve, that the ferroelectric part of the hysteresis loop is not really linear and that we have used ceramic samples in which a complete saturation of the dielectric polarization is not obtained. However the results prove the reliability of the calculations of ΔG_1 from EP curves.

An estimation of the activation energy ΔG_2 for the transition $\beta_t \rightarrow FE_t$ can be obtained from the virgin hysteresis loops. This is illustrated in Figs. 7 and 10, where the shaded region corresponds to the activation energy ΔG_2, being the maximum amount of energy stored in the material (corrected for the dielectrically stored energy). A plot of ΔG_2 as a function of temperature is constructed in Fig. 9 for two different materials. For *PLZT* 17/30/70 it can be seen, that on lowering the temperature the activation energy decreases and eventually ΔG_2 becomes so small, that the transition $\beta \rightarrow FE$ occurs spontaneously.

PLZT 20/30/70 shows a different behaviour. On lowering the temperature, the activation energy decreases, but around the temperature T_p no further decrease is observed and a constant value of about 1.5 cal/mol is obtained. A further lowering of the temperature eventually leads to an increase of the activation energy to rather high values. For microregions with linear dimensions of 100 Å (volume $v = 10^6$ Å$^3 \approx 2.5 \times 10^{-20}$ mol) the values of V. ΔG_2 are large in comparison with the average thermal energy kT and in our opinion this activation energy will prevent the spontaneous occurance of the $\beta \rightarrow FE$ transiton and will be the reason for the temperature difference between the *real* (calculated) transition temperature T_0 and the *observed* transition temperature T_p for the transition $FE_t \rightarrow \beta_t$. The origin of the large activation energy in these materials is not yet clear.

3.3 *Heat effects during the electrically induced* $\beta_t \rightarrow FE_t$ *conversion*

In this section it will be shown that the field-induced $\beta_t \rightarrow FE_t$ transition is accompanied by an exothermic heat-effect, which supports the ideas, developed in the previous sections.

If the material is FE, the heat liberated during poling is very small, but if the material is in the β_t state, a notable heat-effect is observed during poling. This heat-effect appears to be in good agreement with the endothermic heat-effect, observed during the depoling of the material at temperature T_p.

Our *DSC* equipment is essentially the same as the one Keve and Annis used for their experiments [3]. Ceramic discs with evaporated gold electrodes were used. Fine platinum leads connected the sample in the *DSC* cell to an external power supply. Measurements were made on several materials at temperatures $T < T_p$. Since the heat effect involved in the $FE_t \rightarrow \beta_t$ transition at T_p is endothermic (Section 2), we expected the opposite, field induced, transition to be exothermic. Applying an electric field + V to thermally depoled material indeed resulted in the expected exothermic heat-effect Q_1. This heat-effect must be corrected for the electrical heat dissipation and for the reversibly stored dielectric energy (Q_2). Furthermore a calibration of the *DSC* peaks should be made.

The calibration of the *DSC* peaks is carried out by measuring the heat-effects during a complete EP hys-

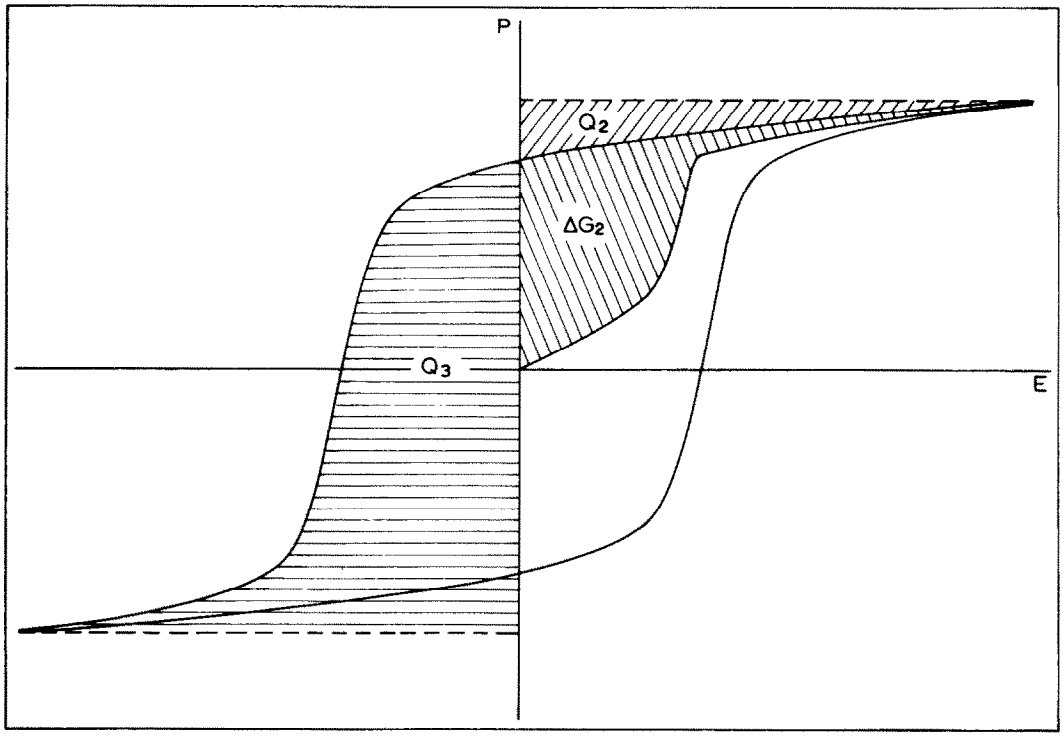

Fig. 10. Calculation of the activation energy ΔG_2, the reversibly stored dielectric energy Q_2 and the energy Q_3 from a square hysteresis loop.

teresis loop. On reducing the electric field $+V$ (or $-V$) to a short-circuit condition, an endothermic heat-effect Q_2 is observed. This heat effect is equivalent to the reversibly stored dielectric energy shown in Fig. 10.

Subsequent application of an electric field $-V$ resulted in an exothermic heat-effect Q_3. The physical meaning of Q_3 is also shown in Fig. 10.

It can be deduced from this figure, that the total heat dissipation in a complete EP hysteresis loop is given by 2 $(Q_3 - Q_2)$ and since this heat-effect can be determined quite accurately from the EP hysteresis measurements, we have a method to calibrate the *DSC* peaks.

Finally the electrical heat dissipation during the transition $\beta_t \rightarrow \mathrm{FE}_t$ can be determined from the *virgin* EP curve and is equivalent to the activation energy ΔG_2 (Section 3.2, see also Fig. 10).

In conclusion it can be stated, that the corrected transition heat involved in the conversion $\beta_t \rightarrow \mathrm{FE}_t$ is given by Q_1 minus the reversibly stored dielectric energy Q_2 and minus the activation energy ΔG_2. In Fig. 11 this corrected heat-effect during poling is given for several materials as a function of temperature. More reproducible results were obtained when the experiments were carried out at temperatures not too close to the temperature T_p.

It can be seen that for materials that do not show a spontaneous transition to the FE phase (x/30/70 with $x > 18$ at % La), a more or less constant value of Q in a large temperature interval $T < T_p$ is observed. This value of Q proves to be in good agreement with the other *DSC* results (Table 1) and with the results of the hysteresis measurements.

A quite different behaviour is seen for *PLZT* 17/30/70. At low temperatures, the material is already ferroelectric and only a small heat-effect is observed during poling. Increasing the temperature eventually leads to a transition $\mathrm{FE}_t \rightarrow \beta_t$ at the temperature T_s (see Part I of this paper).

Applying an electric field to the material at temperatures $T_s < T < T_p$ results in a non reversible transition $\beta_t \rightarrow \mathrm{FE}_t$ and the value of Q increases rapidly. The small heat-effect observed at *low* temperatures may be due to a non-complete spontaneous conversion β-FE in the thermally depoled material. Further it can be stated, that the observed exothermic heat-effect during poling again points to a field induced transition. It should be

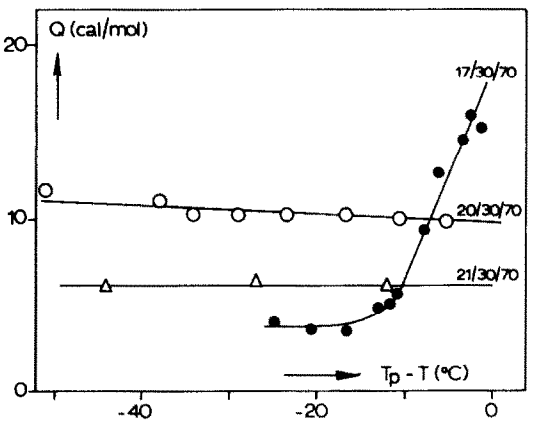

Fig. 11. Transition heat as a function of temperature for *PLZT* x/30/70 materials.

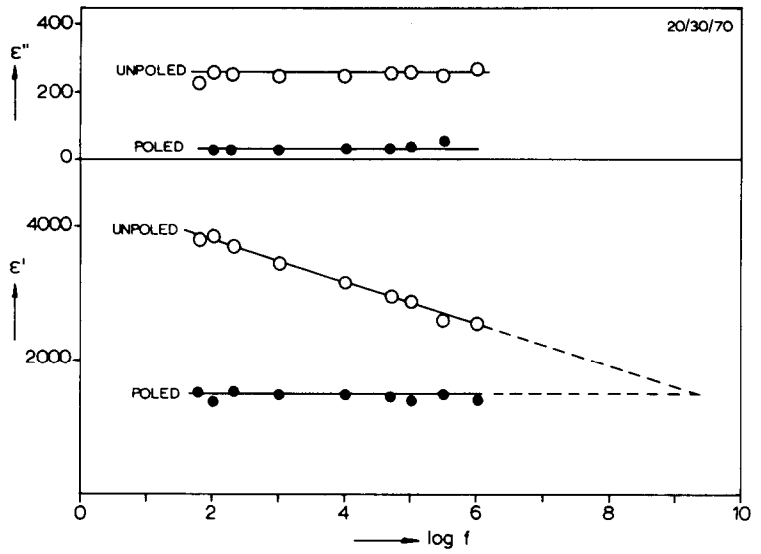

Fig. 12. Frequency dependence of the dielectric constant and the dielectric loss at −90°C for *PLZT* 20/30/70 (f in Hz).

kept in mind however that in this way the heat-effects for the transition from the β_t phase to the *poled* FE_t phase were determined. A correction for the domain orientation process was not performed.

3.4 *Frequency dependence of the β phase*

To estimate whether the observed decrease in dielectric constant after poling is related to normal domain processes, we have measured the frequency dependence of the dielectric constant and dielectric loss of *PLZT* 20/30/70 at −90°C. It can be seen from Fig. 12, that at low frequencies there is an extra contribution to the dielectric constant and dielectric loss, which can be removed by poling. As the measuring frequency increases the extra contribution to the dielectric constant becomes smaller. If it is allowed to extrapolate the curves to high frequencies it can be concluded, that somewhere in the *GHz* range the dielectric constants of poled and unpoled material become equal. This suggests, that the extra contribution to the dielectric constant in unpoled material could be due to a domain wall relaxation. However the dielectric loss for unpoled material does not show the expected maximum as frequency increases†.

In conclusion it can be stated that the fact that we have observed a strongly dispersive dielectric constant together with a *non dispersive dielectric loss* in a frequency range 100 Hz-1 MHz does not point to normal domain processes.

Similar effects have been observed in $KSr_2Nb_5O_{15}$ (KSN) crystals by Clarke and Burfoot [13] and in $Ba_{0.5}Sr_{0.5}Nb_2O_6$ crystals by Cline and Cross [14]. In KSN the dielectric constant for unpoled materials is strongly dispersive and $\epsilon'_{unpoled} \gg \epsilon'_{poled}$. In this case a maxinum in the dielectric loss as function of frequency is observed at about 10^4 Hz. The phenomena in KSN are explained by a model, which assumes the existence of microdomains seperated by thick (50Å) domainwalls. In our opinion this model is closely related to the short range order model discussed in Part II of this paper.

3.5 *Thermal hysteresis*

In our opinion, the effects observed in *PLZT* materials with a high La content are related to thermal hysteresis. In a previous section it was made clear, that in *PLZT* 17/30/70 a more or less normal, though large, thermal hysteresis for the transition $\beta_t \leftrightarrows FE_t$ is observed. In zero field the transition $\beta_t \rightarrow FE_t$ occurs on cooling at temperature T_a (Fig. 6), whereas the opposite transition takes place on heating at temperature T_b. This thermal hysteresis is caused by a rather large activation energy, as can be seen from Fig. 9. In *PLZT* 20/30/70 the situation is not essentially different. In this case however the activation energy exhibits a minimum as a function of temperature.

At low temperatures this activation energy is so large, that a spontaneous $\beta_t \rightarrow FE_t$ transition does not occur. One can say that the thermal hysteresis has become infinite in this case. Measurements on *PLTZ* 19/30/70 and 21/30/70 materials showed that the $\Delta G_2(T)$ curves are qualitatively similar to the one that is shown in Fig. 9. for *PLZT* 20/30/70. However the minimum value of ΔG_2 increases rapidly with increasing La content. The minimum values are 1 and 2.5 cal/mol for 19/30/70 and 21/30/70 respectively.

In conclusion it can be stated, that in *PLZT* materials, the $\beta_t \leftrightarrows FE_t$ transition is accompanied by an unusual thermal hysteresis. This unusual character is phenomenologically expressed by the fact that the thermal hysteresis becomes infinite for materials with a high La content. This so called "infinite" thermal hys-

†It should be remarked, that at high (>300 kHz) and low (<200 Hz) frequencies the accuracy of the ϵ'' measurements is not better than 15%. It is possible that a very broad maximum can be observed in this frequency range if more accurate measurements are carried out. Moreover the frequency range in our measurements is rather limited.

teresis" is probably not caused by nucleation problems. To understand this it should be kept in mind that both the β-phase and the FE phase are tetragonal. In the short range order model (see Part II of this paper) the β-phase is considered as a phase with FE microdomains and therefore it is illogical to suppose that a nucleation problem prevents the spontaneous transition $\beta_t \rightarrow FE_t$.

Finally the difference in character between the $\beta \leftrightarrows PE$ transition and the $FE \rightleftarrows \beta$ transition is remarkable. The transition $\beta \leftrightarrows PE$ is very diffused, without any thermal hysteresis, whereas the transition $\beta \leftrightarrows FE$ is a much "sharper" transition with an unusual thermal hysteresis. Only in *PLZT* 21/30/70 is some diffuseness of the $FE_t \rightarrow \beta_t$ transition observed.

3.6 *Comparison with other* PLZT *materials*

Tetragonal *PLZT x*/55/45 materials were investigated extensively by Wolters *et al.* [7]. In these materials the phenomenon of inducing a FE phase by means of an electric field was also observed. In this case a distinction between β_t and FE_t phases can also be made [6, 7] and the transition $\beta_t \rightarrow FE_t$ has the same characteristics (exothermic heat-effect during poling, anomalous decrease of ϵ' during poling, etc.) as in the case of *PLZT x*/30/70 materials. As has been illustrated by our results on 11/55/45, shown in Table 1, the transition $\beta_t \rightarrow FE_t$ in *PLZT x*/55/45 materials is of first order and a large temperature difference is observed between the real transition temperature T_0 and the actual transition temperature T_p. Just as in the case of *PLZT x*/30/70 materials with $x > 18$ at % La, the transition $\beta_t \rightarrow FE_t$ does not occur spontaneously in *PLZT* 11/55/45 and a determination of the activation energy ΔG_2 (see Section 3.2) as a function of temperature results in a $\Delta G_2(T)$ curve, which is qualitatively similar to the one observed for *PLZT x*/30/70 materials.

The broad minimum in the $\Delta G_2(T)$ curve is observed in the temperature region 0–50°C and the minimum value is about 1 cal/mol. This large activation energy (with respect to the average thermal energy) will prevent the spontaneous occurance of the $\beta_t \rightarrow FE_t$ transition.

By comparison with the *x*/30/70 series, one can see, that an increase of the Ti content leads to an increase of the La concentration range where a classical $Fe_t \rightarrow PE_c$ transition is observed and an increase of the La content is necessary for observing a field induced $\beta_t \rightarrow FE_t$ transition. In *PLZT* 11/55/45 for example, the FE phase only forms after poling, but in *PLZT* 11/30/70 no such behaviour is observed. Field induced transitions are observed in *PLZT x*/30/70 materials for $x > 16$ at % La.

Increasing the Ti content still more, eventually leads to a situation observed in PLT. In these materials a more or less classical $FE_t \rightarrow PE_c$ transition occurs up to very high La concentrations [9]. A notable broadening of the maximum in the $\epsilon'(T)$ curve is observed for $x = 30$ at %La, but an induction of the FE phase is not observed.

Also in non-tetragonal *PLZT* materials, the induction of a FE phase by means of an electric field is possible. The situation in *PLZT x*/65/35 materials is reviewed shortly in the introduction and a field induced cubic → orthorombic transition is observed in *PLZT x*/65/35 materials for $x > 7$ at % La. Finally in *PLZT x*/85/15 materials a non-reversible field induced AFE → FE transition is observed [10]. In conclusion it can be stated, that the electrical induction of a FE phase is a universal phenomenon in *PLZT* materials. However the La concentration at which this phenomenon is observed and the characteristics of the field induced transition are different for different parts of the phase diagram.

Unfortunately, little is known about the value of the transition heat for the field induced transition in other *PLZT* materials. Keve and Annis [3] determined a transition heat of 8 cal/mol for *PLZT* 8/65/35. This value is in the same order of magnitude as the values that have been observed for tetragonal *PLZT* materials (12 cal/mol for *PLZT* 11/55/45 and 6–20 cal/mol for *PLZT x*/30/70 materials dependent on *x*). A comparison with some other polar → non-polar transitions has been made in Table 2. It can be seen that the heat-effects involved in the field induced transitions *PLZT* materials are small.

A final remark must be made with respect to the β_t phase. Wolters [7] regarded the β_t phase in *PLZT x*/55/45 materials as AFE, but the evidence for antiferroelectricity was rather poor and in *PLZT x*/30/70 materials no AFE properties were observed. In our opinion the short range order model is the more likely model. In this model, described in more detail in [4] and [6], a ferroelectric phase with short range order develops spontaneously from the paraelectric phase in the temperature region, where the permittivity curve exhibits a broad-

Table 2. Transition enthalpies (ΔH) and entropies (ΔS) of some ferroelectric and antiferroelectric compounds

material	transition temp (K)	ΔH (cal/mol)	ΔS (cal/molK)	transition	ref.
$PbTiO_3$	763	1150	1,51	FE→PE	11
$KNbO_3$	708	190	0,28	FE→PE	11
$BaTiO_3$	393	47	0,12	FE→PE	11
$PbZrO_3$	503	440	0,88	AFE→PE	11
$Pb(Zr_{0,5}Ti_{0,5})O_3$	666	57	0,09	FE→PE	12
PLT 18	428	24	0,06	FE→PE	this paper
PLZT 17/30/70	320	18	0,06	FE→β	this paper
PLZT 20/30/70	212	10	0,05	FE→β	this paper
PLZT 11/55/45	321	12	0,04	FE→β	this paper
PLZT 8/65/35	328	8	0,02	FE→β(?)	3

maximum. A transition to a FE phase with long range order, occurs only after having applied a strong electric field to the material. It is not clear in this model, whether the field induced transition should be regarded as a real transition or more as a conversion from one ferroelectric state to another.

As has been stated in [6], if the material exhibits a more or less complete FE short-range order, a considerable proportion of the material exists in the domain walls between the ordered ferroelectric microdomains. These domain walls resemble a PE phase and poling will result in a *transition* of these PE walls to a FE phase. This process, together with an alignment of the FE microdomains, results in a FE long-range order.

4. CONCLUSIONS

(1) The phase diagram for poled tetragonal *PLZT* materials was determined. In comparison with the phase diagram for thermally depoled materials, the FE_t phase field has grown at the expense of the β_t phase field.

(2) The transition $\beta_t \leftrightarrows FE_t$ has a first order character and shows an unusual thermal hysteresis behaviour. This thermal hysteresis is caused by an activation energy, which is high in comparison with the average thermal energy kT. For materials with a high La content (x/30/70 materials with $x > 18$ at % La) a minimum in the activation energy was observed as a function of temperature. The minimum value of the activation energy increases with increasing La content and is larger than 1 cal/mol in all cases.

(3) Transition enthalpies and entropies for the transition $\beta_t \leftrightarrows FE_t$ were determined. Results obtained with different methods agree rather well. The transition enthalpy decreases with increasing La content and has a low value (6–20 cal/mol for x/30/70 materials). The transition entropy is more or less independent of the La content in x/30/70 materials ($\Delta S = 0$, 04–, 06 cal/mol K) and has comparable or lower values for known materials with a higher *Zr* content.

(4) The electrical induction of a FE phase is a general phenomenon for the whole *PLZT* system.

Acknowledgements—The present investigations have been carried out under the auspices of the Netherlands Foundation for Chemical Research. (S.O.N.).

REFERENCES

1. Land C. E., Thacher P. D. and Heartling G. H. *Appl. Solid State Sci.* **4**, 137 (1974).
2. Keve E. T. and Bye K. L., *J. Appl. Phys.* **46**, 810 (1975).
3. Keve E. T. and Annis A. D., *Ferroelectrics* **5**, 77 (1973).
4. Carl, K. and Geissen K., *Proc. IEEE* **61**, 59.
5. Meitzler A. H. and O'Bryan H. M., *Proc. IEEE* **61**, 959 (1973).
6. Stenger C. G. F. and Burggraaf A. J., Part I of this paper.
7. Wolters M., Ph.D. Thesis 1976. Twente University of Technology, Enschede The Netherlands.
8. Sawaguchi E., *J. Phys. Soc. Jap.* **8**, 615 (1953).
9. (a) Keizer K. and Burggraaf A. J., *Ferroelectrics* **14**, 671 (1976). (b) Keizer K., Ph.D. Thesis 1976, Twente University of Technology, Enschede. The Netherlands.
10. Thouy G. and Plaetto J., *Bull. Soc. Fr. Cer.* **113**, 71 (1976).
11. Jona F. and Shirane G., *Ferroelectric crystals*, Pergamon Press (1962).
12. Weirauch D. F., Ph.D. Thesis 1968, University of Illinois, Urbana, Illinois 61803, U.S.A.
13. Clarke R. and Burfoot J. C., *J. Phys. D: Appl. Phys.* **8**, 1115 (1975).
14. Cline T. W. and Cross L. E., *J. Appl. Phys.* **49**, 4298 (1978).